EFFECT OF SPACE WEATHERING ON THE IRON OXIDATION STATE OF RYUGU SAMPLES, A STEM-EELS STUDY. P-M. Zanetta[1], M. S. Thompson[2], T. J. Zega[1], T. Noguchi[3], H. Yurimoto[4], T. Nakamura[5], H. Yabuta[6], N. Naraoka[7], R. Okazaki[7], K. Sakamoto[8], S. Tachibana[9], S. Watanabe[10], Y. Tsuda[8], and the Hayabusa2 Min-Pet Fine Sub-team. (zanetta@arizona.edu), [1]Lunar and Planetary Laboratory, University of Arizona, [2]Purdue University, Department of Earth, Atmospheric, and Planetary Sciences; [3]Division of Earth and Planetary Sciences, Kyoto University, [4]Department of Earth and Planetary Sciences, Hokkaido University, [5]Department of Earth Science, Graduate School of Science, Tohoku University, [6]Earth and Planetary Systems Science Program, Hiroshima University, [7]Department of Earth and Planetary Sciences, Kyushu University, [8]Institute of Space and Astronautical Science, Japan Aerospace Exploration Agency, [9]UTokyo Organization for Planetary and Space Science, University of Tokyo [10]Department of Earth and Environmental Sciences, Nagoya University.

Introduction: Japan Aerospace Exploration Agency (JAXA)'s Hayabusa2 mission successfully sampled the surface of asteroid Ryugu and returned 5.4 g of material to Earth on December 6, 2020. The petrography of the most common grains, closely related to the CI chondrites, indicates that asteroid Ryugu experienced severe aqueous alteration. The returned material consists of a fine-grained, phyllosilicate-rich matrix with magnetite, sulfides, sulfates and carbonates. Additionally, among the sampled material are particles containing evidence for space weathering [1]. Such weathering results from solar-wind irradiation and micrometeoroid bombardment which can modify the morphology, microstructure, chemistry, and spectral properties of grains on the surface of airless bodies.

The physical and chemical response of different types of materials in chondrites to space weathering remains poorly understood. Sheet silicates in particular, which dominate the mineralogy of CI chondrites [2], are understudied and are characterized by complex reflectance spectra. Variations induced by space weathering on the iron oxidation states contained in phyllosilicates (as well as the presence of intimately associated fine-grained Fe-rich mineral) may modify significantly the absorption bands and the overall reflectance measured by remote-sensing instruments [3]. Mapping the $Fe^{3+}/\Sigma Fe$ ratio while monitoring the location of the intermingled phases is therefore essential. Here we report on spatially resolved measurements of the oxidation state of Fe determined by electron energy-loss spectroscopy (EELS) in one of the returned samples from asteroid Ryugu that contains evidence of space weathering [4].

Method: We were allocated a section of particle A0058 from JAXA prepared using focused-ion-beam (FIB) methods. The grain was collected at the first touchdown site. The FIB section was analyzed using a 200 keV Hitachi HF5000 aberration-corrected scanning transmission electron microscope (S/TEM) located in the Kuiper Materials Imaging and Characterization Facility (KMICF) at the Lunar and Planetary Laboratory, University of Arizona. The HF5000 is equipped with a cold-field emission gun, a third-order spherical aberration corrector, bright- and annular-dark-field STEM imaging detectors, and two spectrometers: (1) an Oxford Instruments X-Max 100 TLE EDS system including twin, 100-mm^2 silicon-drift detectors and (2) a Gatan GIF Quantum ER electron energy-loss spectrometer (EELS). The microscope was operated with a STEM condenser aperture of 35 μm, a 330 pA probe current, and convergence angle (α) of 28 mrad. Spectra were acquired using a 100 pm probe, and a collection angle (β) of 63 mrad by using high-angle EELS mode, which provides a shorter camera length than standard EELS mode. Spectra were acquired using an EELS entrance aperture of 5 mm, a 0.25 eV/ch dispersion. Maps were acquired by averaging multiple passes (3 frames) a relatively large pixel time of 0.2 s for core loss and 0.001 s for the low loss.

We also measured standards of FeO, Fe_2O_3, and Fe_3O_4 for reference to Fe^{2+}, Fe^{3+}, and mixed Fe^{2+}/Fe^{3+}, respectively, under the same conditions to compare with our measurements and quantify the $\Sigma Fe^{3+}/Fe^{2+}$ ratio. Both the standards and natural samples were processed in the same way. First, a power law background was subtracted using a fitting range of 100 eV, then we subtracted the continuum intensity beneath the edge using a double arctan function as described by [5]. The peak positions were calibrated by fixing the Carbon π* peak energy at 285 eV. Plural inelastic scattering was removed by the Fourier-ratio deconvolution method [6]. The Fe L_{3a} and Fe L_{3b} peak maxima of FeO and Fe_2O_3 were shifted at to 708.7eV and 710.25 eV respectively by systematically applying an offset of 3.19 eV in order to match the energies described in [7]. A spectrum image was acquired over an area measuring 76 × 20 pixels and 2.83 × 0.75 μm which spanned both the space weathered melt deposit and the unaltered matrix. We quantified the Fe $L_{2,3}$ edge using the methods modified by [8] rather than the white line ratio calibration curve developed by [5] because the sample contains minor Fe and is beam sensitive. We obtained a calibration curve similar to [8] and applied this calibration to each pixel of the spectrum image to determine the $Fe^{3+}/\Sigma Fe$ map.

Results and discussion: Bright-field (BF) and high-angle annular-dark-field (HAADF) imaging shows that the matrix material contains phyllosilicates, Fe- and Fe-Ni-sulfide, magnetite, and large carbonate grains. The melt layer described by [4] measures from 300 nm to 3 µm and is mainly composed of Mg-rich amorphous silicates with embedded Fe-bearing particles (mostly sulfides) and vesicles ≤500 nm (Fig.1a).

A HAADF image and corresponding EELS spectrum image of the surface of section A0058 is shown in Fig. 1. Three zones are identified: Region 1 is the phyllosilicate-rich matrix; Region 2 is a mixture of the phyllosilicates in the matrix and a weathered iron sulfide grain; Region 3 is the surface silicate melt layer formed via space weathering. Vesicles and porosity are avoided when defining the zones for quantitative analysis of the oxidation state.

Region 1 contains the highest Fe^{3+} content with values ranging from 50±3% to 80±4% that compare favorably with phyllosilicates from matrices of carbonaceous chondrites [8]. Region 2 shows the lowest Fe^{3+} content. Finally, Region 3 corresponds to a significantly lower Fe^{3+} content in comparison to the matrix material, but higher than Region 2. The average $Fe^{3+}/\Sigma Fe$ values of region 1, 2, and 3 are 68±4%, 28±3% and 40±3% respectively. These values compare favorably with experiments of particles exposed to ion irradiation that show the amorphization of the phyllosilicates to a depth of ~200 nm, void development, and a decrease in the $Fe^{3+}/\Sigma Fe$ ratio in the irradiated layer compared to unirradiated material [9-10].

The results presented here demonstrate that micrometeoroid bombardment affects the iron oxidation state of phyllosilicates. The presence of intimately associated fine-grained Fe-rich minerals add to the complexity. Given that most of our understanding of asteroid surfaces comes from remote sensing data, it is critically important to explore the details of how compositional variation affects spectral features of phyllosilicates. Comparison with STXM studies might also be useful to monitor the beam effect on the oxidation state of this sensitive material.

References: [1] Thompson, M. S., et al. (2020) Icarus, 346, 113775. [2] Tomeoka, K. & Buseck P.R. (1988) *Geochimica et Cosmochimica Acta* 52.6: 1627-1640. [3] Cloutis, E. A., et al. (2011) *Icarus* 212.1:180-209. [4] Thompson, M. S., et al. (2022) *this meeting*. [5] Van Aken, P. A., & Liebscher, B. (2002). *Physics and Chemistry of Minerals,* 29(3), 188-200. [6] Egerton, R. F., & Malac, M. (2005). *Journal of Electron Spectroscopy and Related Phenomena*, 143(2-3), 43-50. [7] Bourdelle, F., et al. (2013). *Contributions to Mineralogy and Petrology,* 166(2), 423-434. [8] Le Guillou, C., et al. (2015). *Earth and Planetary Science Letters,* 420, 162-173. [9] Keller, L. P., & R. Christoffersen, *LPI Contributions* 2189 (2019) abstract #2131. [10] Laczniak, D. L., et al. (2021) *Icarus* 364:114479.

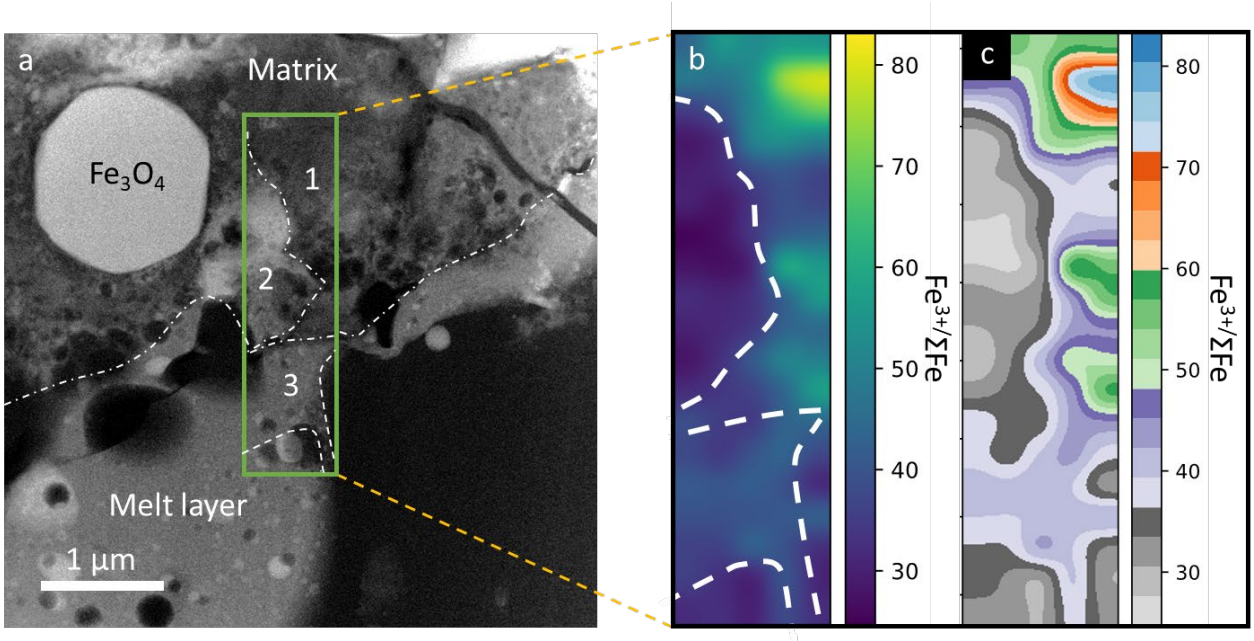

Fig.1: a) STEM-HAADF image of particle A0058. The interface between the matrix and the melt layer is indicated. b) $Fe^{3+}/\Sigma Fe$ map determined from the Fe $L_{2,3}$ edges. c) False-color contour map of the $Fe^{3+}/\Sigma Fe$ distribution.